physical sciences forum

MDPI

Proceeding Paper

The Morphology of the Active Galactic Nucleus and its Impact on Accretion Flows and Relativistic Jets †

Mohammed B. Al-Fadhli

College of Science, University of Lincoln, Lincoln LN6 7TS, UK; malfadhli@lincoln.ac.uk or mo.fadhli7@gmail.com

† Presented at the 2nd Electronic Conference on Universe, 16 February–2 March 2023; Available online: https://ecu2023.sciforum.net/.

Abstract: The G2 gas cloud motion data and the scarcity of observations on the event horizon-scale distances have challenged the comprehensiveness of the central supermassive black hole model. In addition, the recent Planck Legacy 2018 release has confirmed the existence of an enhanced lensing amplitude in the cosmic microwave background power spectra. Notably, this amplitude is higher than that estimated by the lambda cold dark matter model, which prefers a positively curved early Universe with a confidence level higher than 99%. This study investigates the impact of the background curvature and its evolution over the conformal time on the formation and morphological evolution of central compact objects and the consequent effect on their host galaxies. The formation of a galaxy from the collapse of a supermassive gas cloud in the early Universe is modelled based on interaction field equations as a 4D relativistic cloud-world that flows and spins through a 4D conformal bulk of a primordial positive curvature considering the preference of the Planck release. Owing to the curved background, this scenario of galaxy formation reveals that the core of a galaxy undergoes a forced vortex formation with a central event horizon leading to opposite vortices (traversable wormholes) that spatially shrink while evolving in the conformal time. It indicates that the galaxy and its core are formed in the same process whereas the surrounding gas clouds form the spiral arms due to the frame-dragging induced by the fast-rotating core. It demonstrates that the accretion flow onto the central supermassive compact object only occurs at the central event horizon of the two opposite vortices while their other ends eject the relativistic jets. This can elucidate the relativistic jet formation and the G2 gas cloud motion if its orbit is around one of the vortices but at a distance from the central event horizon. The gravitational potential of the early curved bulk could contribute to galaxy formation while the present spatial flatness deprives the potential of bulk which could lead to galaxy quenching. The formation of a galaxy and its core simultaneously could explain the growth of the supermassive compact galaxy core to a mass of ~10^9 $M_\odot$ at just 6% of the current Universe age.

Keywords: galaxy formation; conformal spacetime; brane-world modified gravity

Citation: Al-Fadhli, M.B. The Morphology of the Active Galactic Nucleus and its Impact on Accretion Flows and Relativistic Jets. *Phys. Sci. Forum* **2023**, *3*, x. https://doi.org/10.3390/xxxxx
Published: 15 February 2023

1. Introduction

Relativistic jets are extended beams of ionized matter that are emitted in opposite directions along the axis of rotation of active galaxies, quasars, stellar black holes, neutron stars and pulsars at speeds that approach the speed of light. Their radiative signatures and kinetic luminosity can be immensely powerful and such jets can exceed thousandths to millions of parsecs in length. The precise mechanisms by which the relativistic jets are produced are under ongoing debate in the scientific community [1–3].

The Planck Legacy 2018 (PL18) release confirmed the presence of an enhanced lensing amplitude in the CMB power spectra, which prefers a positively curved early Universe with a confidence level higher than 99% [4,5]. Albeit the spatial flatness could be

recovered by combining the CMB lensing and baryon acoustic oscillation (BAO) data, concerns were raised regarding the reliability of this combination because the curvature parameter tension between them was measured to be 2.5 to 3σ [6]. In contrast, the closed Universe can naturally explain the anomalous lensing amplitude, aid a large-scale cut-off in primaeval density fluctuations [4] and agree with the low CMB anisotropy observations [7,8].

This study presents a new galaxy formation scenario by utilizing interaction field equations in which celestial objects are considered as 4D relativistic cloud-worlds that flow and spin through a 4D conformal bulk of a primordial curvature considering the preference of PL18 release. The derived model reveals a new mechanism of relativistic jet generation.

2. Interaction Field Equations

The PL18 release has preferred a positively curved early Universe, that is, is a sign of a primordial background curvature or a curved bulk. To incorporate the bulk curvature and its evolution over the conformal time, a modulus of spacetime deformation, E_D in terms of energy density, is introduced based on the theory of elasticity [9]. The modulus can be expressed in terms of the resistance of the bulk to the localized curvature induced by celestial objects by using Einstein field equations or in terms of the field strength of the bulk by using the Lagrangian formulation of the energy density existing in the bulk as a manifestation of the vacuum energy density as follows

$$E_D = \frac{T_{\mu\nu} - T g_{\mu\nu}/2}{R_{\mu\nu}/\mathcal{R}} = \frac{-\mathcal{F}_{\lambda\rho}\mathcal{F}^{\lambda\rho}}{4\mu_0} \tag{1}$$

where $\mathcal{F}_{\lambda\rho}$ is the field strength tensor of the bulk and μ_0 is vacuum permeability. By incorporating the bulk influence, the Einstein–Hilbert action can be extended to

$$S = E_D \int_C \left[\frac{R}{\mathcal{R}} + \frac{L}{\mathcal{L}}\right]\sqrt{-g}\; d^4\rho \tag{2}$$

where $R = R_{\mu\nu}g^{\mu\nu}$ is Ricci scalar curvature representing a localized curvature induced in the bulk by a celestial object that is regarded as a 4D relativistic cloud-world of metric g_{uv} and Lagrangian density $L = L_{\mu\nu}g^{\mu\nu}$. $\mathcal{R} = \mathcal{R}_{\mu\nu}\tilde{g}^{\mu\nu}$ is the scalar curvature of the 4D bulk of metric $\tilde{g}_{\mu\nu}$ whereas $\mathcal{L} = \mathcal{L}_{\mu\nu}\tilde{g}^{\mu\nu}$ is the bulk's Lagrangian density as an indication of its internal stresses and momenta reflecting its curvature. A dual-action concerning the conservation of energy on global (bulk) and local (cloud-world) scales can be introduced as

$$S = \int_B \left[\frac{-\mathcal{F}_{\lambda\rho}\tilde{g}^{\lambda\gamma}\mathcal{F}_{\gamma\alpha}\tilde{g}^{\rho\alpha}}{4\mu_0}\right]\sqrt{-\tilde{g}}\; \int_C \left[\frac{R_{\mu\nu}g^{\mu\nu}}{\mathcal{R}_{\mu\nu}\tilde{g}^{\mu\nu}} + \frac{L_{\mu\nu}g^{\mu\nu}}{\mathcal{L}_{\mu\nu}\tilde{g}^{\mu\nu}}\right]\sqrt{-g}\; d^4\rho\; d^4\sigma \tag{3}$$

By applying the principle of stationary action in [10] yields

$$\frac{R_{\mu\nu}}{\mathcal{R}} - \frac{1}{2}\frac{R}{\mathcal{R}}g_{\mu\nu} - \frac{R\mathcal{R}_{\mu\nu}}{\mathcal{R}^2} + \frac{R\left(\mathcal{K}_{\mu\nu} - \frac{1}{2}\mathcal{K}\hat{q}_{\mu\nu}\right) - \mathcal{R}\left(K_{\mu\nu} - \frac{1}{2}K\hat{q}_{\mu\nu}\right)}{\mathcal{R}^2} = \frac{\hat{T}_{\mu\nu}}{\mathcal{T}_{\mu\nu}} \tag{4}$$

The interaction field equations can be interpreted as indicating that the cloud-world's induced curvature over the bulk (background) curvature equals the ratio of the cloud-world's imposed energy density and its flux to the bulk's vacuum energy density and its flux in the expanding/contracting Universe. By comparing Equation (1) with Einstein field equations, which gives $\mathcal{T}_{\mu\nu} \coloneqq E_D = \mathcal{R}c^4/8\pi G_{\mathcal{R}}$, the equations can be simplified to

$$R_{\mu\nu} - \frac{1}{2}R\hat{g}_{\mu\nu} - (K_{\mu\nu} - \frac{1}{2}K\hat{q}_{\mu\nu}) = \frac{8\pi G_{\mathcal{R}}}{c^4}\hat{T}_{\mu\nu} \tag{5}$$

where $\hat{g}_{\mu\nu} = g_{\mu\nu} + 2\mathcal{R}_{\mu\nu}/\mathcal{R} + 2\bar{\bar{g}}_{\mu\nu}$ or can be expressed as $\hat{g}_{\mu\nu} = g_{\mu\nu} + 2\tilde{g}_{\mu\nu} + 2\bar{\bar{g}}_{\mu\nu}$ is the conformally transformed metric counting for the contributions of the cloud-world metric, $g_{\mu\nu}$, in addition to the contribution from intrinsic and extrinsic curvatures of the bulk,

whereas Einstein spaces are a subclass of conformal spaces [11]. The evolution in $G_{\mathcal{R}}$ reflects the field strength of the bulk and depends on the bulk or background curvature.

3. Galaxy Formation and Relativistic Jet Generation

The entire contribution comes from the boundary term when calculating the black hole entropy using the semiclassical approach [12,13]. By applying this concept and rearranging the field equations for this setting as

$$R_{\mu\nu} - \frac{1}{2}Rg_{\mu\nu} - \frac{R\mathcal{R}_{\mu\nu}}{\mathcal{R}} = \frac{8\pi G_{\mathcal{R}}}{c^4}\hat{T}_{\mu\nu} - \frac{R\left(\mathcal{K}_{\mu\nu} - \frac{1}{2}\mathcal{K}\hat{q}_{\mu\nu}\right) - \mathcal{R}\left(K_{\mu\nu} - \frac{1}{2}K\hat{q}_{\mu\nu}\right)}{\mathcal{R}} = 0 \tag{6}$$

The field equations can describe the interaction between a 4D relativistic cloud-world of intrinsic $R_{\mu\nu}$ and extrinsic $K_{\mu\nu}$ curvatures with a stress-energy $\hat{T}_{\mu\nu}$ and the 4D bulk of intrinsic $\mathcal{R}_{\mu\nu}$ and extrinsic $\mathcal{K}_{\mu\nu}$ curvatures with a stress-energy $\mathcal{T}_{\mu\nu}$. From Equation (6), the field equations yield

$$R_{\mu\nu} = \frac{1}{2}Rg_{\mu\nu} + \frac{R\mathcal{R}_{\mu\nu}}{\mathcal{R}} = \frac{1}{2}R\left(g_{\mu\nu} + 2\tilde{g}_{\mu\nu}\right) = \frac{1}{2}Rg_{\mu\nu}(1 + 2\Omega^2) = 0 \tag{7}$$

where $\hat{g}_{\mu\nu} = g_{\mu\nu} + 2\tilde{g}_{\mu\nu}$ and $\tilde{g}_{\mu\nu} = \mathcal{R}_{\mu\nu}/\mathcal{R} = \mathcal{R}_{\mu\nu}/\mathcal{R}_{\mu\nu}\tilde{g}^{\mu\nu}$ is the conformal bulk metric, which can be expressed as proportional to cloud-world metric $g_{\mu\nu}$ as $\tilde{g}_{\mu\nu} = g_{\mu\nu}\Omega^2$ by utilizing Ω^2, the conformal transformation function. The conformally transformed metric $\hat{g}_{\mu\nu} = g_{\mu\nu}(1 + 2\Omega^2)$ can be expressed as

$$ds^2 = -A(r)\left(1 + 2\Omega^2(r,\mathcal{r})\right)c^2dt^2 + S^2\left(B(r)\left(1 + 2\Omega^2(r,\mathcal{r})\right)dr^2 + r^2d\theta^2 + r^2sin^2\theta\, d\phi^2\right) \tag{8}$$

where A and B are functions of the cloud-world radius r, S^2 is a dimensionless conformal scale factor. By performing the coordinate transformation as follows

$$ds^2 = -\left(A(\lambda) + 2A(\lambda)\Omega^2(\lambda,\mathcal{r})\right)c^2dt^2 + \left(B(\lambda) + 2B(\lambda)\Omega^2(\lambda,\mathcal{r})\right)d\lambda^2 + \lambda^2d\theta^2 + \lambda^2sin^2\theta\, d\phi^2 \tag{9}$$

where the conformal function Ω^2 is a function of the bulk radius of curvature $\mathcal{r}$ and it can be influenced by the cloud-world radius.

The Christoffel symbols of this metric are

$$\Gamma^1_{00} = \frac{\dot{A}(1 + 2\Omega^2) + 4A\dot{\Omega}}{2(B + 2B\Omega^2)}, \quad \Gamma^0_{01} = \frac{\dot{A}(1 + 2\Omega^2) + 4A\dot{\Omega}}{2(A + 2A\Omega^2)}, \quad \Gamma^1_{11} = \frac{\dot{B}(1 + 2\Omega^2) + 4B\dot{\Omega}}{2(B + 2B\Omega^2)}$$

$$\Gamma^1_{22} = \frac{-\lambda}{(B + 2B\Omega^2)}, \quad \Gamma^1_{33} = \frac{-\lambda sin^2\theta}{(B + 2B\Omega^2)}, \quad \Gamma^2_{21} = \Gamma^2_{12} = \frac{1}{\lambda} \tag{10}$$

$$\Gamma^2_{33} = -\,sin\theta\, cos\theta, \quad \Gamma^3_{32} = \Gamma^3_{23} = \frac{cos\theta}{sin\theta}$$

where the sign $\dot{}$ is a total derivative of the function. The Ricci tensor components are

$$R_{tt} = -\frac{\frac{d}{d\lambda}\left(\dot{A}\left(1 + 2\Omega^2\right) + 4A\dot{\Omega}\right)}{2\left(B + 2B\Omega^2\right)} - \frac{\dot{A}\left(1 + 2\Omega^2\right) + 4A\dot{\Omega}}{2\left(B + 2B\Omega^2\right)}\frac{\dot{B}\left(1 + 2\Omega^2\right) + 4B\dot{\Omega}}{2\left(B + 2B\Omega^2\right)}$$
$$+ \frac{\dot{A}\left(1 + 2\Omega^2\right) + 4A\dot{\Omega}}{2\left(B + 2B\Omega^2\right)}\frac{\dot{A}\left(1 + 2\Omega^2\right) + 4A\dot{\Omega}}{2\left(A + 2A\Omega^2\right)} - \frac{1}{\lambda}\frac{\dot{A}\left(1 + 2\Omega^2\right) + 4A\dot{\Omega}}{2\left(B + 2B\Omega^2\right)} \tag{11}$$

$$R_{tt} = -\frac{\ddot{A}\left(1 + 2\Omega^2 + 4\dot{\Omega}\right) + 4A\ddot{\Omega} + 4\dot{\Omega}\dot{A}}{2\left(B + 2B\Omega^2\right)} + \frac{\left(\dot{A}\left(1 + 2\Omega^2\right) + 4A\dot{\Omega}\right)\left(\dot{B}\left(1 + 2\Omega^2\right) + 4B\dot{\Omega}\right)}{4\left(B + 2B\Omega^2\right)^2}$$
$$+ \frac{\left(\dot{A}\left(1 + 2\Omega^2\right) + 4A\dot{\Omega}\right)^2}{4\left(A + 2A\Omega^2\right)\left(B + 2B\Omega^2\right)} - \frac{1}{\lambda}\frac{\dot{A}\left(1 + 2\Omega^2\right) + 4A\dot{\Omega}}{\left(B + 2B\Omega^2\right)} \tag{12}$$

$$R_{rr} = \frac{1}{2}\left(\frac{\ddot{A}\left(1+2\Omega^2+4\dot{\Omega}\right)+4A\ddot{\Omega}+4\dot{\Omega}\dot{A}}{\left(A+2A\Omega^2\right)} - \frac{\left(\dot{A}\left(1+2\Omega^2\right)+4A\dot{\Omega}\right)^2}{2\left(A+2A\Omega^2\right)^2} \right) - \frac{\left(\dot{A}\left(1+2\Omega^2\right)+4A\dot{\Omega}\right)\left(\dot{B}\left(1+2\Omega^2\right)+4B\dot{\Omega}\right)}{4\left(A+2A\Omega^2\right)\left(B+2B\Omega^2\right)} - \frac{1}{\lambda}\frac{\dot{B}\left(1+2\Omega^2\right)+4B\dot{\Omega}}{B+2B\Omega^2} \quad (13)$$

$$R_{\theta\theta} = \frac{1}{\left(B+2B\Omega^2\right)} - \frac{\lambda}{2\left(B+2B\Omega^2\right)}\left(\frac{\dot{B}\left(1+2\Omega^2\right)+4B\dot{\Omega}}{\left(B+2B\Omega^2\right)} - \frac{\dot{A}\left(1+2\Omega^2\right)+4A\dot{\Omega}}{\left(A+2A\Omega^2\right)} \right) - 1 \quad (14)$$

$$R_{\phi\phi} = \frac{sin^2\theta}{\left(B+2B\Omega^2\right)} - \frac{\lambda sin^2\theta}{2\left(B+2B\Omega^2\right)}\left(\frac{\dot{B}\left(1+2\Omega^2\right)+4B\dot{\Omega}}{\left(B+2B\Omega^2\right)} - \frac{\dot{A}\left(1+2\Omega^2\right)+4A\dot{\Omega}}{\left(A+2A\Omega^2\right)} \right) - sin^2\theta \quad (15)$$

By substituting Ricci tensor components to Equation (7) gives

$$\left(\dot{A}(1+2\Omega^2)+4A\dot{\Omega}\right)(B+2B\Omega^2) + (A+2A\Omega^2)\left(\dot{B}(1+2\Omega^2)+4B\dot{\Omega}\right) = 0 \quad (16)$$

Equation (16) yields

$$B + 2B\Omega^2 = \frac{k}{A+2A\Omega^2} \quad (17)$$

where $k = 1 + 4\Omega^2 + \Omega^4$ for the conformal metric by considering the bulk curvature.

By applying the weak-field limit: $\hat{g}_{\mu\nu} \approx \eta_{\mu\nu} + \hat{h}_{\mu\nu}$, as follows

$$\Gamma^i_{tt} = \frac{1}{2}\int \partial_i \hat{h}_{tt} = \frac{1}{c^2}\int \partial_i \varphi \quad (18)$$

where φ is the Newtonian gravitational potential. By integrating both sides

$$\hat{g}_{tt} = -A(1+2\Omega^2) = -\left(\eta_{tt} + \frac{2\varphi_c}{c^2} + \frac{2\varphi_p}{c^2}\right) \quad (19)$$

where $\varphi_c = -GM/\lambda$ is the gravitational potential of the cloud-world's spherical mass and φ_p that arises from the integration can be interpreted as the gravitational potential resulting from the bulk curvature, which can be expressed, using the same Newtonian analogue, in terms of the mass, M_p, of the early Universe plasma of preferred positive curvature and the bulk curvature radius r as $\varphi_p = -G_p M_p/r$. The metric should yield only the gravitational potential of the cloud-world when there is no bulk curvature $(\Omega^2 = 0)$ and $(\varphi_b = 0)$; hence, $A = (1 + 2\varphi_c/c^2)$; consequently, the conformal function is $\Omega^2 = \varphi_p/Ac^2$.

By performing the coordinate retransformation and combining Equations (17–19) yield

$$\Omega^2 = -\frac{G_p M_p}{rc^2}\left(1 - \frac{2GM}{rc^2}\right)^{-1}, \qquad A = 1 - \frac{2GM}{rc^2}, \qquad B = \left(1 - \frac{2GM}{rc^2}\right)^{-1} \quad (20)$$

where the conformal function Ω^2 relies on the gravitational potential of the bulk while its influence is inversely proportional to cloud-world potential. In the case of PI18's preferred early Universe positive curvature, the gravitational potential of the bulk can be expressed in terms of the early Universe plasma of mass, M_p, and r denoting the radius of curvature of the bulk, where the bulk's potential decreases with the Universe expansion and vanishes in the flat spacetime background ($r \to \infty$). The minus sign of Ω^2 reveals a spatial shrinking through evolving in the conformal time, which agrees with the vortex model that can occur due to high-speed spinning. By substituting Equation (20) to Equation (8), the conformally metric $\hat{g}_{\mu\nu} = g_{\mu\nu} + 2\tilde{g}_{\mu\nu} = g_{\mu\nu}(1 + 2\Omega^2)$ is

$$ds^2 = \left(1 - \frac{r_s}{r} - \frac{\mathcal{r}_p}{\mathcal{r}}\right)\left(-c^2dt^2 + S^2\left(\frac{dr^2}{1 + \frac{r_s{}^2}{r^2} - 2\frac{r_s}{r}} + \frac{r^2d\theta^2 + r^2sin^2\theta d\phi^2}{1 - \frac{r_s}{r} - \frac{\mathcal{r}_p}{\mathcal{r}}}\right)\right) \quad (21)$$

This metric reduces to the Schwarzschild metric in a flat background ($\mathcal{r} \to \infty$), where $\mathcal{r}$ is the background or bulk curvature radius, r_s is Schwarzschild radius, $\mathcal{r}_p = 2G_pM_p/c^2$ is early Universe gravitational radius and S^2 is a dimensionless spatial scale factor. The denominator of the radial dimension can be interpreted as an intrinsic curvature term where the metric on the radial and two-sphere is warped by the bulk and cloud-world radii. The metric can be visualized through evolving in the conformal time by using Flamm's approach as follows

$$w(\mathfrak{r}, r) = \mp \int \frac{\sqrt{\left(\frac{r_s}{r} - \frac{r_s{}^2}{r^2} - \frac{\mathcal{r}_p}{\mathcal{r}}\right)}}{\left(1 - \frac{r_s}{r}\right)} dr = \mp \sqrt{r_s(r - r_s) - \mathcal{r}_p\frac{r^2}{\mathcal{r}}} + \mathcal{O} + C \quad (22)$$

where C is a constant and $\mathcal{O}$ denotes less significant terms. By choosing an appropriate C, Figure 1 shows the proper distances, and their corresponding proper areas are increasing as they are evolving in the conformal time while the radius decreases.

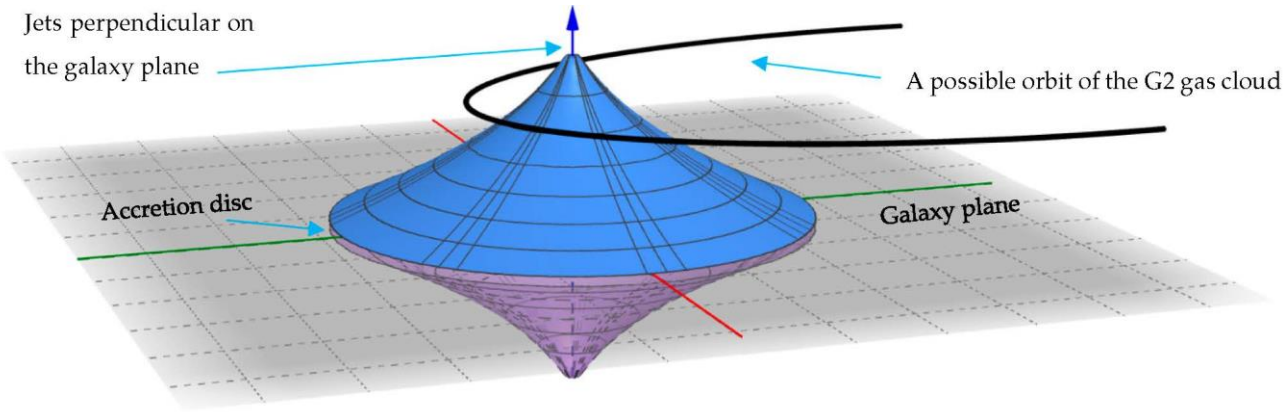

Figure 1. The metric of the supermassive compact object as a central event horizon leading to opposite vortices with two jets that are perpendicular on the rotation plane.

The increase in the proper distances and their corresponding proper areas as the radius decreases agree with the vortex model while the positive and negative solutions of Equation (22) indicate the evolution of the vortex in opposite directions, i.e., forming a dual vortex perpendicular on the galaxy plane. The 4D cloud-world of metric $g_{\mu\nu}$ through its travel and spin in the conformal space-time of the 4D bulk of metric $\tilde{g}_{\mu\nu}$.

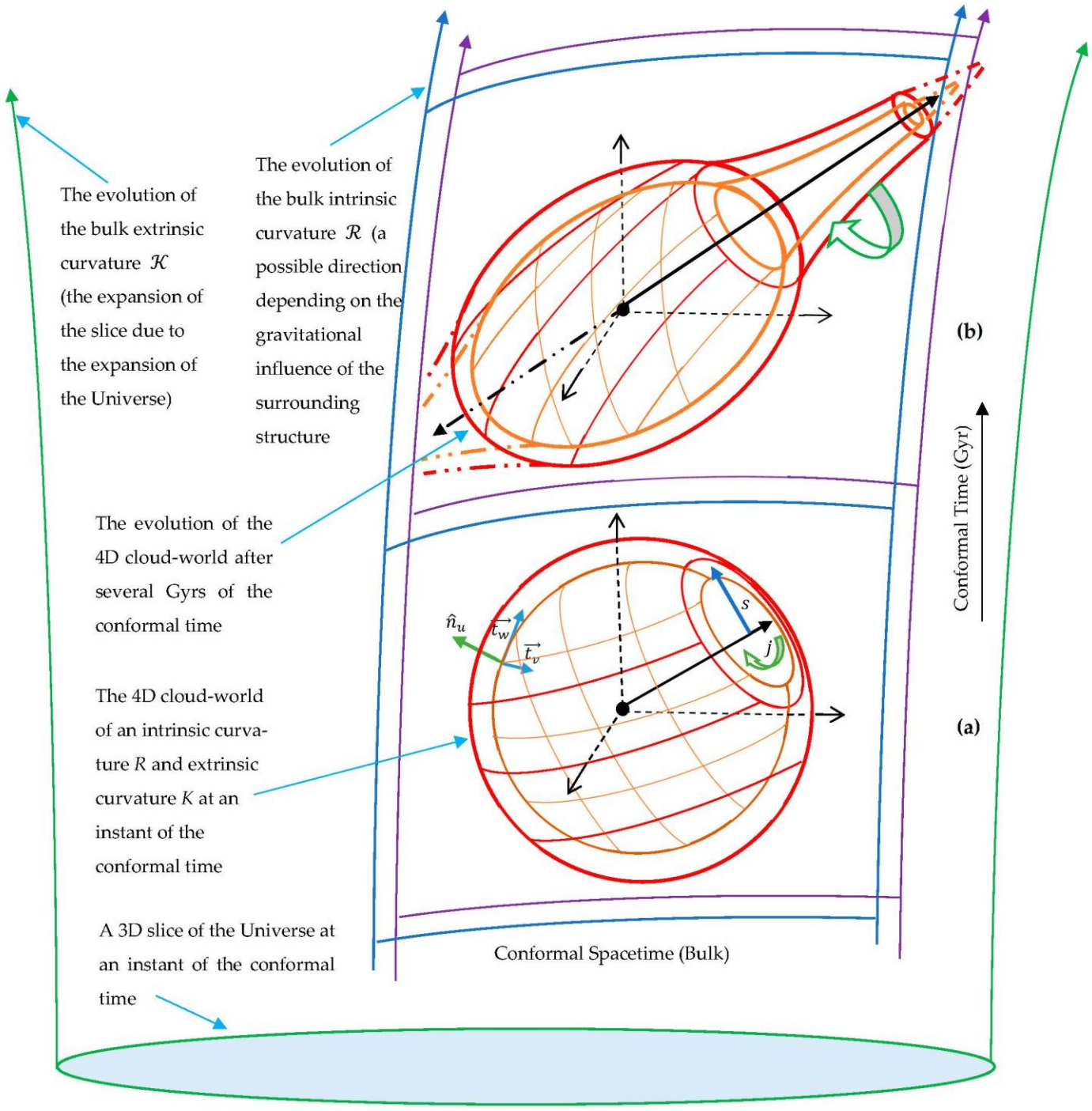

Figure 2. The hypersphere of a compact core of a galaxy (the red-orange 4D cloud-world) along with its travel and spin through the conformal spacetime (the blue-purple 4D bulk representing the bulk of distinctive curvature evolving over the conformal time.

The G2 cloud has only faced drag forces [14,15], where orbiting a vortex could explain these observations if its orbit is at a distance from the central event horizon. In addition, the observations of the superluminal motion in the x-ray jet of M87 [16] could be travelled through these two opposite traversable wormholes.

To evaluate the influence of the spinning and the curvature of the bulk on the core of the galaxy and the surrounding gas clouds (the spiral arms), a fluid simulation was performed based on Newtonian dynamics by using the Fluid Pressure and Flow software [17]. In this simulation, the fluid was deemed to represent the spacetime continuum throughout incrementally flattening curvature paths representing conformal curvature

evolution to analyze the external momenta exerted on objects flowing throughout the incrementally flattening curvatures. The momenta yielded by the fluid simulation were used to simulate a spiral galaxy as a forced vortex as shown in Figure 3.

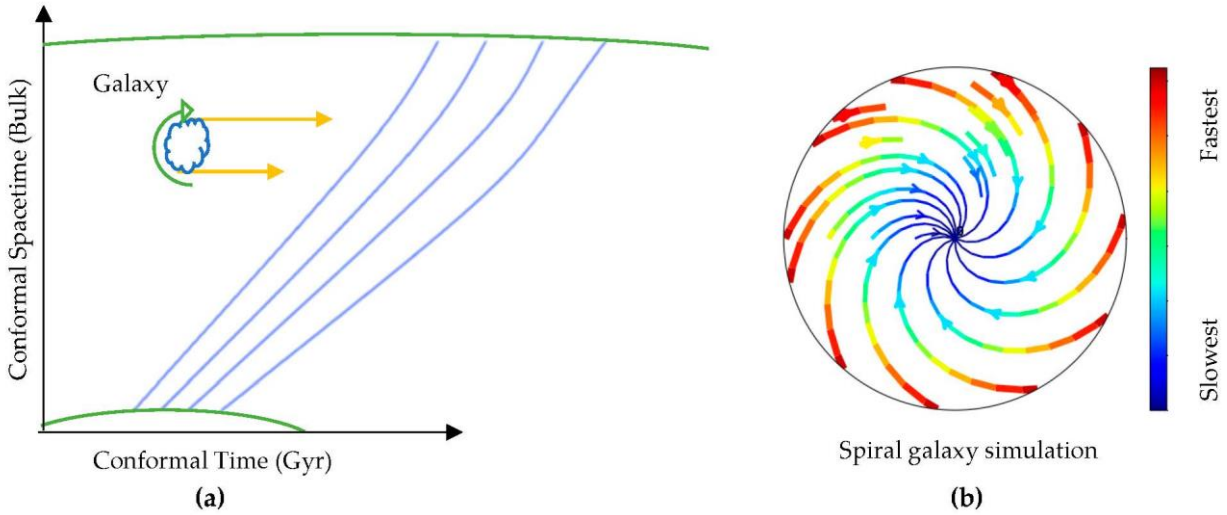

Figure 3. (**a**) External fields exerted on a galaxy due to the spacetime conformal curvature evolution. Green curves represent the curvature of spacetime worldlines. Blue curves represent the simulated spacetime continuum. (**b**) Simulation of spiral galaxy rotation. Blue represents the slowest tangential speeds and red represents the fastest speeds.

The simulation shows that the tangential speeds of the outer parts of the spiral galaxy are rotating faster in comparison with the rotational speeds of the inner parts, which resembles observations of galaxy rotation except the simulation used an ideal fluid.

4. Conclusions and Future Works

In this study, interaction field equations are derived in which the curvature of the background or the 4D conformal bulk evolves over the conformal time based on the PL18 recent release which has preferred a positively curved early Universe with a confidence level higher than 99%. Throughout this bulk, 4D relativistic cloud-worlds flow and spin.

Owing to the curved background, the findings of galaxy formation showed that the core of the galaxy undergoes a forced vortex formation with a central event horizon leading to opposite traversable wormholes that are spatially shrinking through evolving in the conformal time. It revealed that the galaxy and its core form in the same process, while the surrounding gas clouds can form spiral arms due to the fast-rotating core. These findings demonstrated that the accretion flow onto the central supermassive compact object only occurs at the central event horizon of the two opposite vortices while their other ends eject the relativistic jets. The formation of the galaxy and its core at the same process can explain the formation of supermassive compact galaxy cores with a mass of ~10^9 $M_\odot$ at just 6% of the current Universe age and could solve the black hole hierarchy problem.

References

1. Beall, J.H. A Review of Astrophysical Jets. *Front. Res. Astrophys. II* **2016**, *mbhe 58*, 53.
2. Kundt, W. A Uniform Description of All the Astrophysical Jets. *PoS (FRAWS 2014)*, **2014**, *25*, 1–9.
3. Beall, J.H. A review of astrophysical jets. In *Frascati Workshop 2013, Proceedings of the The Tenth International Workshop on Multifrequency Behaviour of High Energy Cosmic Sources Palermo, Italy, 2013*; Naval Research Laboratory, Washington, DC, USA, 2014; pp. 259–264.
4. Di Valentino, E.; Melchiorri, A.; Silk, J. Planck evidence for a closed Universe and a possible crisis for cosmology. *Nat. Astron.* **2020**, *4*, 196–203.
5. Mokeddem, R.; Hipólito-Ricaldi, W.S.; Bernui, A. 2022 Excess of lensing amplitude in the Planck CMB power spectrum. *J. Cosmol. Astropart. Phys.* **2023**, *1*, 017.

6. Handley, W. Curvature tension: Evidence for a closed universe. *Phys. Rev. D* **2021**, *103*, L041301.
7. Linde, A. Can we have inflation with Omega > 1? *J. Cosmol. Astropart. Phys.* **2023**, *2003*, 002.
8. Efstathiou, G. Is the Low CMB Quadrupole a Signature of Spatial Curvature? *Mon. Not. R. Astron. Soc.* **2003**, *343*, 0–000.
9. Landau, L.D. *Theory of Elasticity*; Elsevier: Amsterdam, The Netherlands, 1986.
10. Al-Fadhli, M.B. 2022 Celestial and Quantum Propagation, Spinning, and Interaction as 4D Relativistic Cloud-Worlds Embedded in a 4D Conformal Bulk: From String to Cloud Theory. *Preprints* **2020**, 2020100320. https://doi.org/10.20944/preprints202010.0320.v9.
11. Kozameh, C.; Newman, E.; gravitation, K.T.-G. *Conformal Einstein Spaces*; Springer: Berlin/Heidelberg, Germany, 1985.
12. Dyer, E.; Hinterbichler, K. Boundary terms, variational principles, and higher derivative modified gravity. *Phys. Rev. D Part. Fields, Gravit. Cosmol.* **2009**, *79*, 024028.
13. Brown, J.D.; York, J.W. Microcanonical functional integral for the gravitational field. *Phys. Rev. D* **1993**, *47*, 1420–1431.
14. Burkert, A.; Schartmann, M.; Alig, C.; Gillessen, S.; Genzel, R.; Fritz, T.K.; Eisenhauer, F. Physics of the galactic center cloud G2, on its way toward the supermassive black hole. *Astrophys. J.* **2012**, *750*, 58.
15. Becerra-Vergara, E.A.; Argüelles, C.R.; Krut, A.; Rueda, J.A.; Ruffini, R. Hinting a dark matter nature of Sgr A* via the S-stars. *Mon. Not. R. Astron. Soc. Lett.* **2021**, *505*, L64–L68.
16. Snios, B.; Nulsen PE, J.; Kraft, R.P.; Cheung, C.C.; Meyer, E.T.; Forman, W.R.; Jones, C.; Murray, S.S. Detection of Superluminal Motion in the X-Ray Jet of M87. *Astrophys. J.* 2019 , 879, 8.
17. Reid, S.; Podolefsky, H.; Pual, A. *Fluid Pressure and Flow, PhET Interactive Simulations*; University of Colorado: Denver, CO, USA, 2013.